

专任教师岗位低职高聘聘任申请表

姓 名	钱亨	出生年月	1992 年 4 月	参加工作时间	2020 年 11 月
现所在单位	机械学院	最高学历/学位	博士	现聘专业技术职务	助教
现校聘岗位	专业技术九级	取得学历/学位时间	2020 年 8 月	聘任专业技术职务时间	2020 年 11 月
现省聘岗级	<input checked="" type="checkbox"/> 专业技术岗 IX 级 <input type="checkbox"/> 管理岗 _____ 级				
拟申请岗位	(机械学院专任教师副高级Ⅶ级)		校聘岗位类别	(教学科研并重型)	
是否按照专技身份享受校内绩效政策（双肩挑人员填写）			<input type="checkbox"/> 是 <input type="checkbox"/> 否		
任现职（岗级）以来取得业绩	A 类项目：___项				
	B 类项目：_1_项	SCI 论文			
	C 类项目：___项				
	业绩换算分值		4		
本人承诺	<p>本人知悉《第四轮岗位聘用实施办法》、《校内绩效工资实施方案》、《浙江水利水电学院“三定”方案（2020 版）》、《第四轮岗位聘任工作实施方案》等文件规定和各单位（部门）岗位聘任实施方案、岗位说明书，经慎重考虑申请相应岗位。承诺：</p> <p>1、以上所填内容全部属实，如有问题本人愿意承担一切责任；</p> <p>2、受聘岗位期间，能够履行相关文件要求及岗位说明书规定的岗位职责。</p> <p style="text-align: right;">本人签名： <u>钱亨</u></p> <p style="text-align: right;">2021 年 4 月 21 日</p>				
以上部分由申请人填写，应聘部门审核。以下由单位（部门）和管理服务岗位聘用委员会填写。					
原单位（部门）意见	<div style="display: flex; justify-content: space-between; align-items: center;"> <div> <input type="checkbox"/> 同意 <input type="checkbox"/> 不同意 </div> <div style="text-align: right;"> （部门盖章） ____年__月__日 </div> </div>				

应聘单位（部门）聘任意见	<div>1、经审核，申请人所填内容：<input type="checkbox"/>属实 <input type="checkbox"/>不属实</div> <div>2、是否符合所申请岗位的申报条件：<input type="checkbox"/>符合 <input type="checkbox"/>不符合</div> <div>3、是否同意聘任所申请岗位：<input type="checkbox"/>同意 <input type="checkbox"/>不同意</div> <div>(部门盖章)</div> <div>____年____月____日</div>
专任教师岗位聘用委员会意见	<div>专任教师岗位聘用委员会主任委员签名：_____</div> <div>____年____月____日</div>

备注：表格请用 A4 纸打印，与聘岗有关佐证材料附后。

Investigation of Self-Priming Process of a Centrifugal Pump with Double Blades

QIAN Heng¹, MOU Jiegang², REN Yun³, ZHU Zhibing¹, LIU Nuoja¹, ZHENG Shuihua¹, WU Denghao^{2*}

1. College of Mechanical Engineering, Zhejiang University of Technology, Hangzhou 310014, China

2. College of Metrology & Measurement Engineering, China Jiliang University, Hangzhou 310018, China

3. Zhijiang College, Zhejiang University of Technology, Shaoxing 312030, China

© Science Press, Institute of Engineering Thermophysics, CAS and Springer-Verlag GmbH Germany, part of Springer Nature 2020

Abstract: The gas-liquid two-phase flow patterns of a centrifugal pump during the self-priming process were investigated numerically and experimentally. The Euler-Euler multiphase model and SST $k-\omega$ turbulence model were applied for simulating the self-priming process. Meanwhile, the change of motor speed and self-priming height were considered in the simulation. The overall transient two-phase flow features and water level distributions were mapped. Results showed that the self-priming process was divided into three stages. The liquid level in inlet-pipe rose in oscillation during self-priming process. The variations of water level during self-priming process of numerical simulation and test result agreed well. The inlet-pipe (Ver) was filled at 22 s and 24 s respectively numerically and experimentally. The bubble cloud circulated in the volute during middle stage of self-priming process, and breakup into smaller bubbles by shear force and tongue, and then discharged into chamber. The bubbles in the outlet-pipe mainly included bubbly flow and slug flow at the last stage of self-priming process, which is morphologically consistent with the test results. Also, during the self-priming process, the reflux liquid was pressed by blades and fully mixed with gas; that is the way to realizing the function of self-priming.

Keywords: self-priming process, gas-liquid two-phase flow, centrifugal pump, gas-liquid mixing and separation, transient numerical simulation

1. Introduction

Self-priming pump is widely used in municipal engineering, agricultural engineering, architectural engineering, and petrochemical industries due to its self-priming capacity. Currently, the application of numerical simulation in hydraulic performance design has become more and more mature [1–4]. However, the numerical simulation has not been widely applied to study the self-priming performance of centrifugal pump

due to its poor prediction accuracy and huge computation resources. Besides, the gas-liquid two-phase distribution in self-priming pump is extremely complex, and the mechanism of gas-liquid mixing and separation was not fully understood. Also, the design method for the improvement of self-priming capacity is still not fully developed, which restricts the development of self-priming pumps.

Currently, many studies were undertaken to understand the flow patterns of centrifugal pump during the

Nomenclature

b_2	blade outlet width/mm	Q_{gs}	gas discharge in simulation/m ³
D_1	impeller inlet diameter/mm	Q_{gt}	gas discharge in test/m ³
D_2	impeller outlet diameter/mm	Ti	impeller revolution/s
H	self-priming height of test/m	V_{inlet}	volume of gas in inlet pipe/m ³
H_d	head of pump/m	V	gas volume/m ³
h	water level rise height/m	V'	changed volume/m ³
L	length of inlet-pipe horizontal/m	z	number of blades
n	rotation speed/r·min ⁻¹	ΔV	gas volume difference between test and simulation/m ³
n_q	specific speed	ΔH	difference value between test and simulation/m
P	pressure/Pa	η	efficiency/%
P'	changed pressure/Pa	ρ	density of the water/kg·m ⁻³
Q_d	flow rate of pump/m ³ ·h ⁻¹	Φ	warp angle/°

self-priming process. The numerical simulation of gas-liquid two-phase flow in self-priming pump was earlier studied based on Mixture model [5–7]. The impeller inlet with different volume fraction of gas was investigated. Results presented that the blade passage is full of bubble cloud with the increase of volume fraction of gas; the suction surface has higher volume fraction of gas than the pressure surface. Li et al. [8, 9] studied the transient gas-liquid two-phase flow field in self-priming pump during self-priming process base on volume of fluid (VOF) model. The rotational speed of the impeller and the pressure curve of the pump outlet from test were set as boundary condition by user-defined function (UDF). The results revealed that the pressure and void fraction experience a rapidly transient process in the start-stage of self-priming process; there is a gas-liquid mixing layer appeared at the outer edge of the impeller. Moreover, high-speed photography system was built to investigate the bubbles in the self-priming pump during self-priming process to verify the accuracy of numerical simulation [10–12]. Huang et al. [13] studied the self-priming process in a conventional vertical self-priming centrifugal pump. The situation of a real world was used as the initial conditions during the simulation, and the voids of gas distributions inside a pump were captured successfully. Li et al. [14–16] studied gas-liquid distribution in the pump chamber during self-priming process in flow-ejecting self-priming pump based on Euler-Euler multiphase model. It was found that the self-priming process improved by adding reinforcing plate on guide vane back. Wang et al. [17] established one suitable numerical method of self-priming process by the weak boundary conditions (pressure inlet and opening outlet). The water levels in the outlet sections of experimental and CFD results were compared to validate the simulation accuracy. The whole self-priming process was divided into 3 stages, and the

middle self-priming stage was the main stage which determined the time of self-priming process. Although the valuable information of gas-liquid two-phase flow distribution in self-priming pump was presented yet, the mechanism of self-priming process and its flow patterns were still not fully uncovered. Also, the simulation method needs to be developed to adapt the different structures of centrifugal pump. Therefore, it is important to establish a numerical simulation method to predict the flow patterns during the self-priming process in the centrifugal pump with double blades.

With the development of multiphase flow model [18] and experimental methods, the gas-liquid two-phase flow and bubble state in centrifugal pump were also researched. Stel et al. [19] studied the motion of bubbles in centrifugal pump impeller numerically and experimentally. The results showed that the discharge speed of bubbles in the impeller is hindered by the increased bubble diameter and impeller speed, but the discharge speed is promoted by the increase of the liquid flow rate. Caridad et al. [20] researched the electrical submersible pump (ESP) under two-phase flow conditions. The phase distribution in the inlet-blade channel was showed by numerical simulation. The hydraulic losses increased because gas pockets destroyed the stable flow, and the larger bubble diameter caused a larger the detriment in head. Zhu et al. [21] studied the flow pattern recognition inside the ESP by transient multiphase simulation. The simulated flow patterns using Eulerian-Eulerian model agree well with the visualization experiments [22]. The flow pattern is dispersed bubble flow in low gas volume fraction, and this causes intermittent/slug flow in large gas volume fraction. Shao et al. [23] revealed the two-phase flow by visualization experiments. The flow patterns in the impeller and volute can be classified into four types with the increasing inlet gas volume fraction (IGVF).

Here, the self-priming process of a centrifugal pump with double blades is studied by transient numerical simulation and experimental test. Main works of this study are as follows: (1) a numerical simulation method is established for predicting the self-priming time of centrifugal pump; (2) comparisons are made for the gas-liquid flow distributions of inlet pipe and outlet pipe between simulation and test; (3) the transient gas-liquid mixing and separation during self-priming process are captured numerically.

2. Numerical Simulation and Experimental Setup

2.1 Experimental setup

In the present work, a self-priming pump with double blades is studied. The main parameters of pump are listed in Table 1. An open-loop self-priming test rig was set up to get the self-priming performance of pump (Fig. 1). The self-priming pump is filled with clean water without any

Table 1 Main data of the self-priming pump

Parameter	Value
Design operation condition	
Flow rate $Q_d/\text{m}^3 \cdot \text{h}^{-1}$	20
Total head H_d/m	20
Rotation speed $n/\text{r} \cdot \text{min}^{-1}$	2900
Specific speed n_q	87
Pump geometrical parameters	
Impeller inlet diameter D_1/mm	60
Impeller outlet diameter D_2/mm	137.5
Blade outlet width b_2/mm	25
Number of blades z	2
Warp angle $\varphi/^\circ$	240
Area of reflux hole S/mm^2	257.1

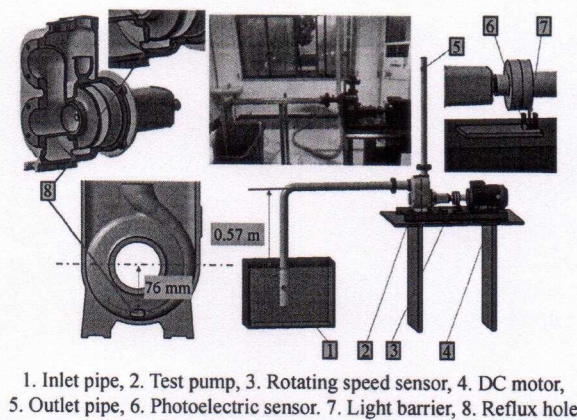


Fig. 1 An open-loop centrifugal pump test rig

impurities by measuring cup before the test and it records the liquid volume for the initial setting of numerical simulation. The change of pump rotating speed is measured by rotating speed sensor and it generates a speed load profile as an input for numerical simulation. The water levels in the inlet and outlet pipes are recorded by a hand-held camera (60 fps).

2.2 Model and mesh

The computational domains of the self-priming pump are constructed and presented in Fig. 2. The test pump mainly consists of S-shape elbow, chamber, volute and impeller. The inlet pipe is divided into two parts for monitoring the water level variation of inlet pipe during self-priming process (the vertical inlet-pipe and horizontal inlet-pipe).

The meshes of fluid domains are created by ANSYS ICEM; the structured hexahedron meshes are generated for inlet-pipe (Ver) and outlet-pipe, and unstructured meshes are generated for the other fluid domains with complex geometries. Mesh refinement is imposed for blades. The grid used for the computational domain is shown in Fig. 2.

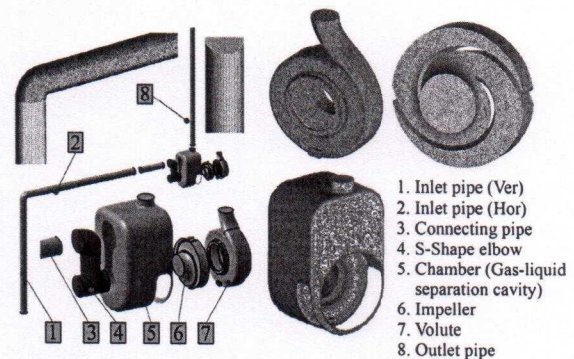


Fig. 2 Computational domains and meshes of test pump

Local mesh sensitivity test and simulation verification performed on ANSYS CFX 18.0. The simulation is based on single phase. The grid independence is investigated under the designed condition as shown in Table 2. The grid refinement follows a certain increase. The head and efficiency are selected to evaluate the effect of the grid number on the final solution. Results show that the head and efficiency are not sensitive for the grid number. More specifically, the relative error of head and the absolute error of efficiency between each scheme fall below 1.5%. Thus, it is considered that further increase of the grid number does not make a significant difference. Grid scheme 3 with the grid number of 3.55×10^6 is utilized as it is the best compromise between the solution accuracy requirements and the available computer resources.

Table 2 Grid independence investigation

Schemes	Grid number/ 10^6	Head, H/m	$(H-H_s)/H_s/\%$	Efficiency, $\eta/\%$	$(\eta-\eta_s)/\eta_s/\%$
1	1.64	22.14	1.05	51.8	1.37
2	2.45	22.1	0.87	51.6	0.98
3	3.55	22	0.41	51.3	0.39
4	4.25	21.91		51.1	

2.3 Boundary conditions and initialization

The weak constraints (pressure inlet and opening outlet) are more suitable at the numerical simulation of self-priming process [17]. Transient rotor stator method is applied to unsteady simulation. The roughness is 0.04 mm according to casting capability.

The liquid volumes in the self-priming pump and the self-priming height are significant impacts on the self-priming time. In this study, we get the liquid volume in the self-priming test by measuring cup, and ensure the water volume in numerical simulation of self-priming pump is consistent with that in test. Meanwhile, the compressibility of gas in inlet-pipe is considered by equivalent exhaust method, and the self-priming height of numerical simulation is calculated as follows:

$$Q_{gs} = Q_{gt} = V_{inlet} \quad (1)$$

$$PV = P'V' \quad (2)$$

$$\Delta V = \frac{P}{P'} \times V - V \quad (3)$$

$$P = \rho g \times 10.34m \quad (4)$$

$$P' = \rho g \times (10.34m - h) \quad (5)$$

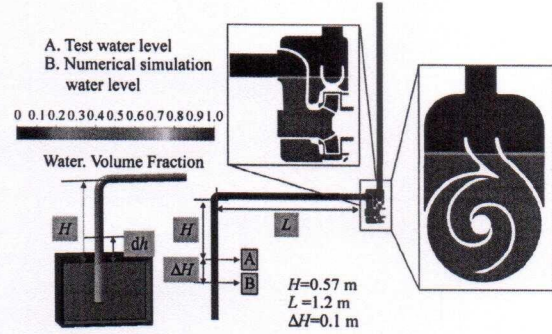
$$\Delta H = \int_0^H \frac{h}{10.34 - h} \times (L + H - h) dh + \frac{H}{10.34 - H} \times L \quad (6)$$

where Q_{gs} is the gas discharged in numerical simulation; Q_{gt} is the gas discharged in test; V_{inlet} is the volume of gas before self-priming process in numerical simulation; P is atmospheric pressure (set as 10.34 m water column); V is gas volume; ρ is density of the water; g is gravitational acceleration; m is meter; h is water level height; H is the self-priming height of test; L is the length of inlet-pipe horizontal; ΔH is the height difference between test and numerical simulation.

The liquid level was initialized before numerical simulation. The impeller center is set as $z=0$ m; the inlet water pipe $z < -0.465$ m is set as water, and the rest is air. S-shaped elbow, volute, chamber and impeller $z < 0.105$ m are set as water. The initialized gas-liquid two-phase state of the self-priming pump is shown in Fig. 3.

2.4 Simulation settings and turbulence model

The unsteady numerical simulation is divided into two steps in order to reveal the gas-liquid two-phase flow distribution during self-priming process in detail. The

**Fig. 3** Initial setting for numerical simulation

liquid-phase contents of different fluid domains of the self-priming pump are monitored. The first step includes the complete self-priming process, total time is set as 90 s and time step is set as 0.005 s. The second step is according to the variation of liquid phase fraction in volute by the numerical simulation result of the first step. The time when liquid phase fraction changes dramatically was chosen to continuous numerical simulation with total time of 0.1 s ($5Ti$: impeller revolution) and time step 2.068×10^{-3} s ($Ti/10$). The second step is mainly to catch the bubble motion during the self-priming process.

The Euler-Euler multiphase model is applied for simulating the self-priming process of pump. The observations from Lu [10] revealed the gas-liquid mixtures are inhomogeneous flow; the gas and liquid are relative motions because of the gas-liquid viscous effect during self-priming process. Hereby, the momentum and continuity equations for the gas and liquid should solve individually. As we known, the VOF model and Mixture model are homogeneous multiphase models and unsuitable to apply them for this simulation. The Euler model is an inhomogeneous multiphase flow, it allowed to solve the momentum and continuity equations for each phase. The SST $k-\omega$ turbulence model is selected for the numerical simulation because of its good behavior in adverse pressure gradients and separating flow [24, 25].

3. Results and Discussion

Fig. 4 shows the liquid phase of different parts during the self-priming process by numerical simulation. The

self-priming process is divided into three stages according to the gas discharge method and flow rate. In the initial stage, the gas of inlet-pipe is sucked into impeller, and the liquid is pumped into volute and chamber. In the middle stage, the gas of inlet-pipe discharged mainly by the gas-liquid mixing and separation process. In the last stage, the gas is discharged together with the liquid during the self-priming process.

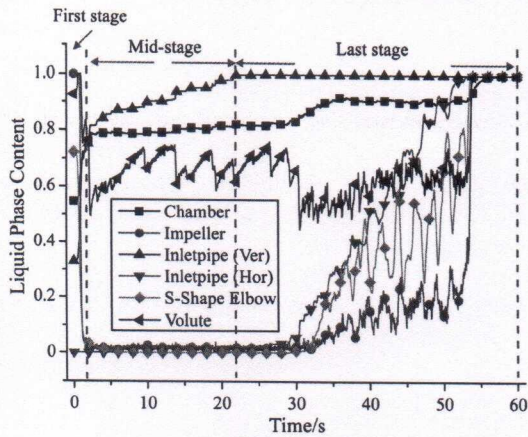
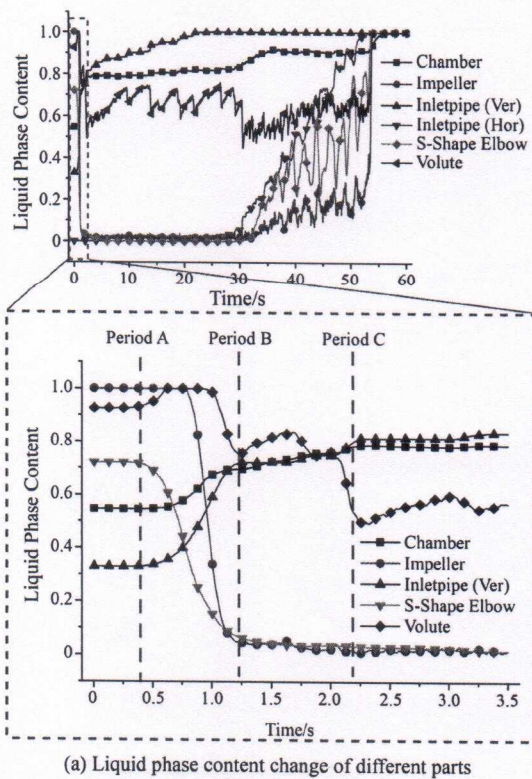


Fig. 4 Liquid phase content change in the self-priming process

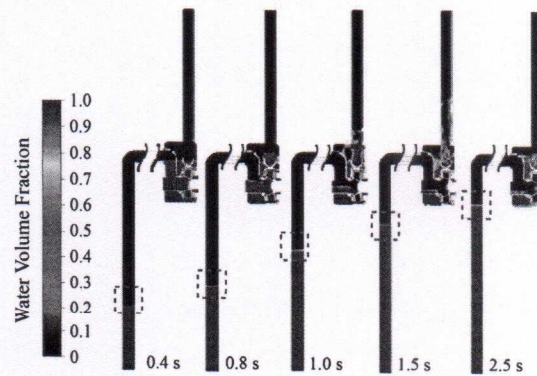


(a) Liquid phase content change of different parts

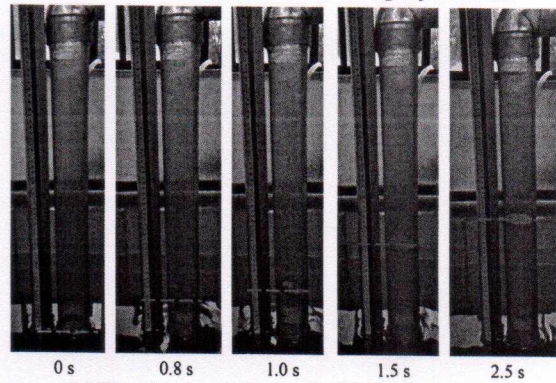
3.1 The initial stage of self-priming process

The initial stage was divided into three periods which shows in Fig. 5(a). Period A is the beginning period (0 s to 0.4 s), the liquid phase content of each part in pump keeps stable. In period B (0.4 s to 1.25 s), the liquid in impeller is discharged and makes the liquid content of volute and chamber increase and the liquid content of S-shape elbow decrease. The liquid content of inlet-pipe (Ver) increases fast until the liquid in S-shape elbow and impeller is exhausted. In period C (1.25 s to 2.25 s), the rising speed of liquid content in inlet-pipe (Ver) is decreased. The results show the liquid phase in inlet-pipe (Ver) increases from 31% to 81% and the liquid phase in impeller decreases from 100% to 2% in the initial stage (0 s to 2.25 s). The liquid phase and gas phase in the inlet-pipe (Ver) keep independent at the initial stage of self-priming process; although the water level in the inlet-pipe (Ver) rises rapidly, there is no mixing between the gas and liquid, and the interface between gas phase and liquid phase is clear. The results of numerical simulation and experiment agree well (Fig. 5(b), Fig. 5(c)).

Fig. 6 shows the details of the gas-liquid distribution in self-priming pump in the initial stage of self-priming process. At 0.8 s, the most zone of S-shape elbow is



(b) Water level variations in the initial stage by numerical



(c) Water level variations in the initial stage by test

Fig. 5 Liquid phase content and water level in initial stage of self-priming process

occupied by gas, and the gas starts to enter the impeller (a in Fig. 6). Water discharges out of volute and falls back to chamber because of the low rotating speed and gravity (b in Fig. 6). At 1.0 s, the water rushes into the outlet-pipe by the increase of rotating speed. With the increase of gas phase content in the impeller, the pressure of liquid drops fast, and water falls down from outlet-pipe after 1.5 s (c in Fig. 6) and then the liquid level keeps steady in chamber.

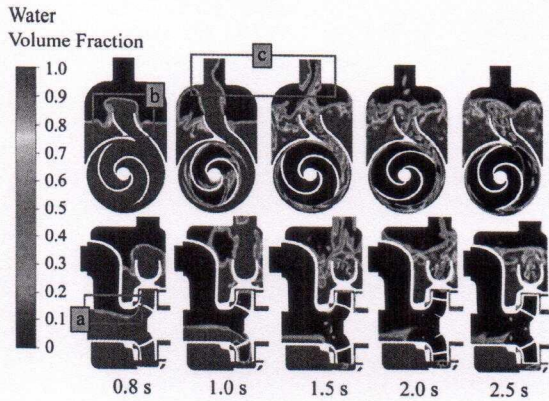
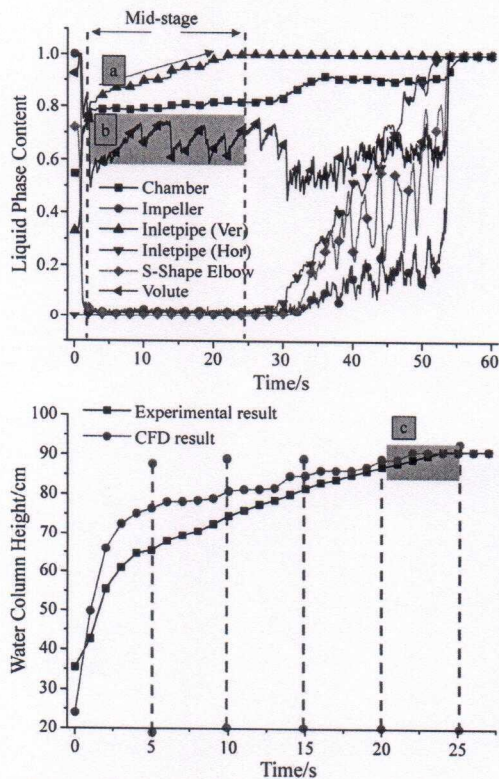


Fig. 6 Gas-liquid distribution details of test pump in first stage of self-priming process

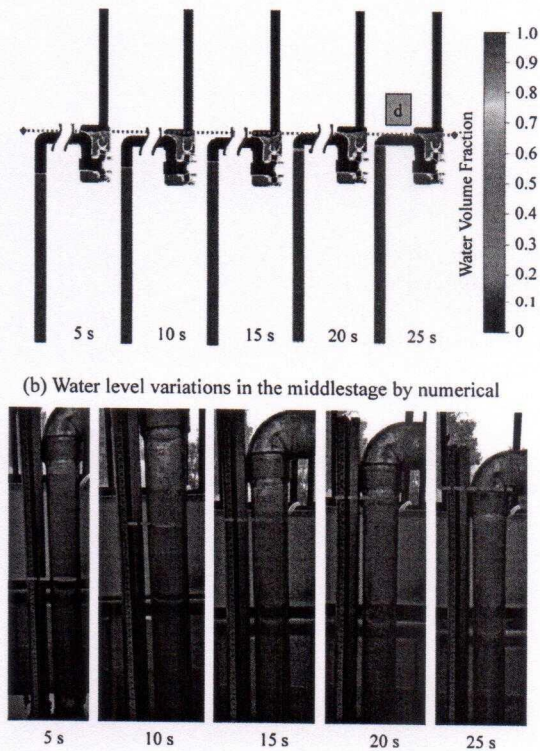


(a) Water column height in inlet-pipe during self-priming process

3.2 The middle stage of self-priming process

Fig. 7 shows the result of calculation and test in the middle stage of self-priming process. In the middle stage (2.25 s to 22 s), the liquid content of inlet-pipe (Ver) slowly increases to 100% (a) and the liquid content of volute fluctuates seriously (b). The gas phase and liquid phase in the impeller mix with each other to form gas-liquid two-phase flow, and then transport to chamber, afterwards gas is separated from gas-liquid mixtures due to the gravity force. The fluctuation in volute shows the discharge of liquid into volute is an intermittent process, and the liquid is discharged when it reaches a certain amount. The separated liquid phase in chamber flows back to the impeller through the reflux hole, and the separated gas is discharged to outlet pipe.

Fig. 7(a) compares the water level changes of inlet-pipe in calculation and test. The increase trend of numerical simulation agrees well with the test results. The height of water column rises significantly in the initial stage of self-priming process and then keeps linear increase until it reaches the top of inlet-pipe. Compared with the test results, outputs from simulation show that the increase of water level is fast in the initial stage and gets slower in the middle stage. The water column reaches the top of inlet-pipe at 22 s in calculation, while



(b) Water level variations in the middlestage by numerical

(c) Water level variations in the middle stage by test

Fig. 7 Liquid phase content and water level in middle stage of self-priming process

it reaches the top of inlet-pipe at 24 s in test (c in Fig. 7(a)). The liquid level in chamber keeps stable during the middle stage (d in Fig. 7(b)).

3.3 The last stage of self-priming process

In the last stage of self-priming process, the liquid from inlet pipe enters into impeller and helps the discharge of gas, which is the key feature in this stage. Normally, as shown in Fig. 8, the liquid is accumulated in the inlet pipe (Hor) for a while, and then it enters into pump at 32 s (a in Fig. 8). The flow in inlet-pipe (Hor) presents wave shape because the intermittent inflow. The liquid content of chamber continuously increases until 36 s because the liquid is discharged to the outlet-pipe (b in Fig. 8). The liquid content of impeller and S-shape elbow rises in fluctuating wave mode in the last stage. The

two-phase flow in outlet-pipe includes bubbly flow and slug flow during the rise of liquid level. Occasionally, gas converges together to form large bubbles and then they are discharged from the outlet-pipe (d in Fig. 8). Afterwards, in the end of the self-priming process, the gas is exhausted completely and the pump runs normally.

Additionally, the liquid is discharged into outlet-pipe at 34 s and takes about 8 s to reach the top of outlet-pipe at 42 s according the calculation result (b and c in Fig. 8). However, the test result presented that the liquid discharged into outlet-pipe at 74 s, and gets the top of outlet-pipe at 80 s. It is found that the self-priming time of test is longer than that of calculation. The self-priming performance is overestimated numerically at the last stage of self-priming process. Some trade-offs were made during the simulation: the viscosity of liquid was ignored;

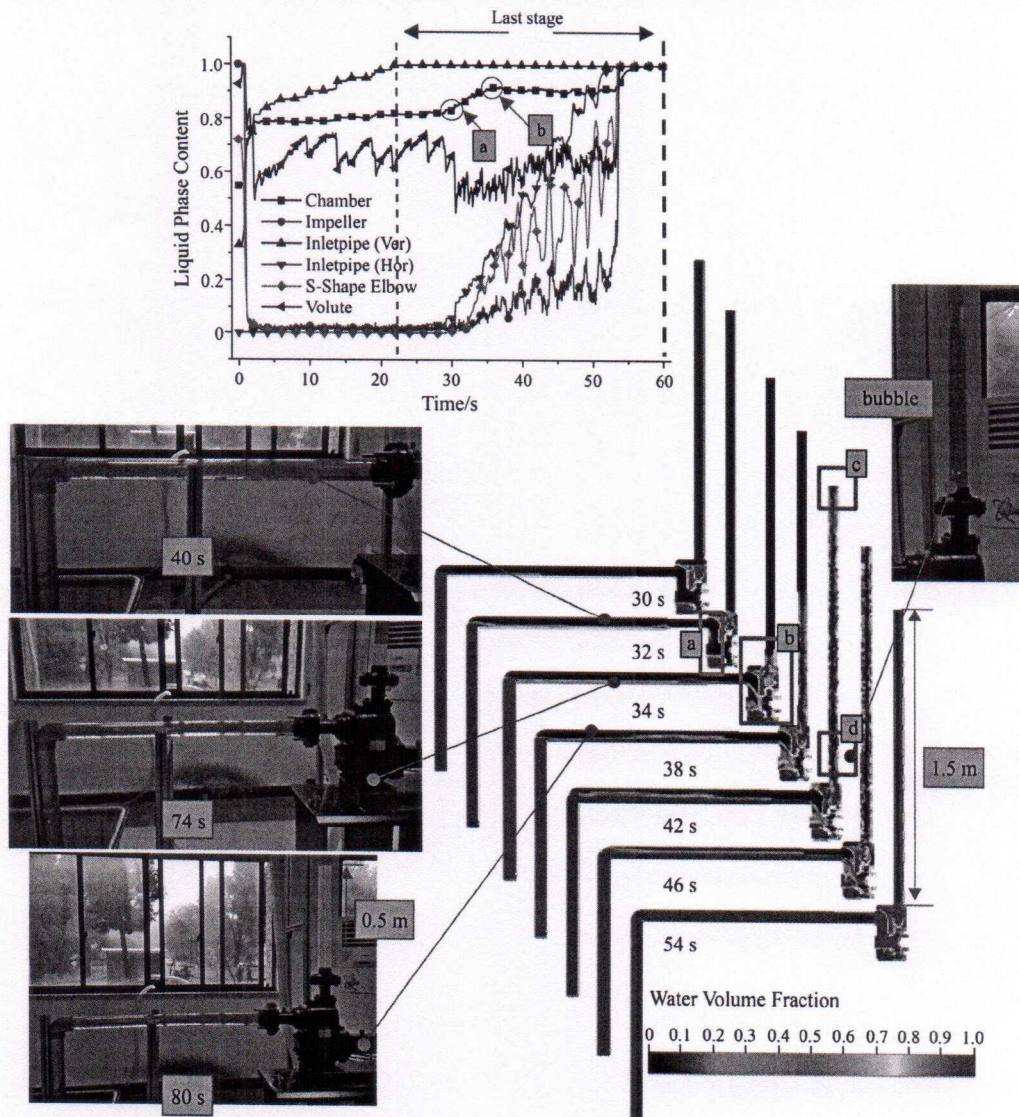


Fig. 8 Liquid phase content and water level in last stage of self-priming process

the mean diameter of bubbles was set as constant; and the drag force of interface between phases was an empirical value, etc. With the improvement of surface treatment technology this year [26–28], the self-priming performance of impeller with surface treatment can be studied in the future.

3.4 Mixing and separation of gas-liquid two-phase flow

The mixing and separation process of gas-liquid two-phase flow are important factors affecting the self-priming performance of pump. Fig. 9 shows the process of gas just enters into impeller and mixes with the liquid in the impeller. The gas enters the impeller from the upper of the impeller inlet, and forms a bubble at the suction side of the blade. The bubble is divided into two parts by the blade (a in Fig. 9). The bubble at the suction grows larger to occupy the blade passage and breaks up again (b in Fig. 9). Some part of bubbles will be separated with the main bubble flow because of the difference of velocities (c1 in Fig. 9). It will breakup into several small bubbles by the impact force of impeller blade (c2 in Fig. 9). Several small bubbles enter into volute due to centrifugal force (c3 in Fig. 9), and are discharged to chamber with the liquid in the volute (c4 in Fig. 9).

Fig. 10 shows the gas discharge process and liquid reflux process in the middle stage of self-priming process. The rate of discharge gas in the middle stage is slower

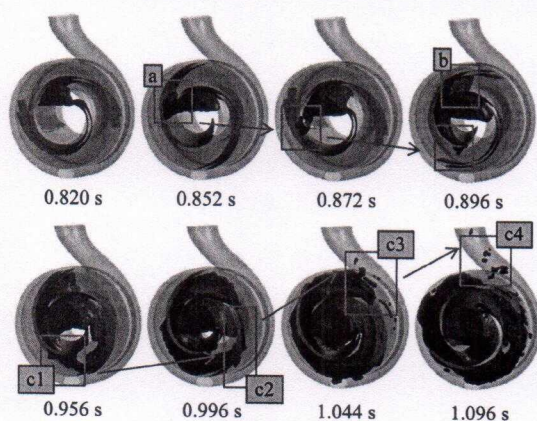


Fig. 9 The process of gas entering into impeller

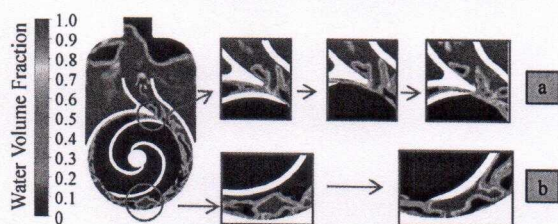


Fig. 10 Gas-liquid mixing and separation in the middle stage

than that in the initial stage. The bubble clouds circulate in the volute with impeller. These bubble clouds and impeller keep the same rotating direction, but the velocity of bubble is much slower than that of impeller. The bubble breaks up when passes through tongue, and some small bubbles are discharged into chamber with liquid and the others are still in the impeller and continue circulating in the volute (a in Fig. 10). The reflux liquid flows back into volute and presses the blade, then fully mixes with gas to generate gas-liquid mixtures (b in Fig. 10).

4. Conclusions

In this paper, the self-priming process of a centrifugal pump with double blades was investigated numerically and experimentally. The conclusions were presented as follows:

(1) The self-priming process was divided into three stages according to the gas discharge method and liquid level state in the test pump. In the initial stage of self-priming process, the liquid contents of different parts were divided into three periods. The liquid phase in the inlet pipe (Ver) increased from 31% to 81%, and the liquid phase in impeller decreased from 100% to 2% in the initial stage (0 s to 2.25 s). The liquid in the impeller was discharged into chamber and volute by the centrifugal force resulting from the impeller rotating, and the negative pressure in impeller inlet and inlet pipe was formed. Therefore, the faster impeller rotating speed led to a lower pressure, and it benefited self-priming performance. The middle stage of self-priming process was a steady gas discharging process. There were three key points which affect the self-priming performance of the pump in the middle stage: the mixing rate of gas and liquid phases in the impeller, the transport rate of gas-liquid mixture to chamber, and the separated rate of gas from liquid phase in the chamber. The liquid level in inlet-pipe rose in fluctuation, and got the peak of the pipe at 24 s. In the last stage of self-priming process, the liquid phase entered into test pump to add the liquid phase fraction in the chamber, increase reflux rate, and keep saturated liquid phase fraction in impeller. This benefited the mixing of the gas and liquid phases in impeller. Eventually, the outlet-pipe was full of liquid, and the gas was discharged to outside by the bubbly and slug flow.

(2) The gas-liquid mixing and separation processes were revealed. The bubble was breakup into several small bubbles by the force from blade, and small bubbles were discharged with liquid. The reflux liquid was pressed by blade and fully mixed with gas to form the liquid-gas mixture.

(3) The numerical methods established in this study

have reference value to predict the time of self-priming process, and the methods could be useful for the other gas-liquid two-phase flow situation. There were still some limitations in this research. In future, the reason of the overestimate of numerical simulation in the self-priming last stage needs to be evaluated, and the accuracy self-priming test needs to be improved with better test facilities.

Acknowledgements

This work was supported by the National Natural Science Foundation of China (51609212, 51606167, 51779226 and 51976193).

References

- [1] Si Q.R., Cui Q.L., Zhang K.Y., Yuan J.P., Bois G., Investigation on centrifugal pump performance degradation under air-water inlet two-phase flow conditions. *Houille Blanche*, 2018, 3: 41–48.
- [2] Ren Y., Zhu Z.C., Wu D.H., Li X.J., Influence of guide ring on energy loss in a multistage centrifugal pump. *Journal of Fluids Engineering-Transactions of the ASME*, 2019; 141: 061302.
- [3] Weme D.G.J.D.O., Schoot M.S.V.D., Kruijt N.P., Zijden E.J.J.V.D., Prediction of the effect of impeller trimming on the hydraulic performance of low specific-speed centrifugal pumps. *Journal of Fluids Engineering-Transactions of the ASME*, 2018, 140: 081202.
- [4] Shim H.S., Kim K.Y. and Choi Y.S., Three-objective optimization of a centrifugal pump to reduce flow recirculation and cavitation. *Journal of Fluids Engineering-Transactions of the ASME*, 2018, 140: 091202.
- [5] Liu J.R., Su Q.Q., Numerical simulation on gas-liquid two-phase flow in self-priming pump. *Transactions of the Chinese Society for Agricultural Machinery*, 2009, 40(9): 73–76.
- [6] Liu J.R., Su Q.Q., Xu Y.G., Wang D.M., Numerical simulation of internal flow field of self-priming irrigation pump. *Journal of Drainage and Irrigation Machinery Engineering*, 2009, 27(6): 347–351.
- [7] Li H., Wang T., Numerical simulation of interior flow and performance prediction for self-priming pump. *Journal of Drainage and Irrigation Machinery Engineering*, 2010, 28(3): 194–197.
- [8] Li H., Xu D.H., Li L., Tu Q., Zhou C.H., Numerical simulation of transient flow in self-priming centrifugal pump during self-priming period. *Journal of Drainage and Irrigation Machinery Engineering*, 2013, 31(7): 565–569.
- [9] Li H., Xu D.H., Tu Q., Cheng J., Li L., Numerical simulation on gas-liquid two-phase flow of self-priming pump during starting period. *Chinese Journal of Mechanical Engineering*, 2013, 29(3): 77–83.
- [10] Lu T.Q., Li H., Zhan L.C., Transient numerical simulation and visualization of self-priming process in self-priming centrifugal pump. *Journal of Drainage and Irrigation Machinery Engineering*, 2016, 34(11): 927–933.
- [11] Li H., Lu T.Q., Zhan L.C., Influence of gap between impeller and tongue on centrifugal pump self-priming performance. *Transactions of the Chinese Society for Agricultural Machinery*, 2017, 48(3): 141–147.
- [12] Li H., Li S.T., Lu T.Q., Transient test and high speed photography research of external mixing self-priming pump. *Journal of Drainage and Irrigation Machinery Engineering*, 2019, 37(5): 375–380.
- [13] Huang S., Su X.H., Guo J., Yue L., Unsteady numerical simulation for gas-liquid two-phase flow in self-priming process of centrifugal pump. *Energy Conversion and Management*, 2014, 85: 694–700.
- [14] Li G.D., Wang Y., Yin G., Cui Y.R., Liang Q.H., Investigation of the self-priming process of self-priming pump under gas-liquid two-phase condition. *Proceedings of the ASME Fluids Engineering Division Summer Meeting*, Illinois, USA, 2014, 21199.
- [15] Wang Y., Li G.D., Cao P.Y., Yin G., Cui Y.R., Li Y.C., Effects of internal circulation flow on self-priming performance of flow-ejecting self-priming pump. *Transactions of the Chinese Society for Agricultural Machinery*, 2014, 45(11): 129–133, 145.
- [16] Li G.D., Wang Y., Mao J.Y. Numerical investigation on the gas-liquid entraining and separating effects on self-priming performance in a flow-ejecting centrifugal pump. *Proceedings of the Institution of Mechanical Engineers, Part A: Journal of Power and Energy*, 2018.
- [17] Wang C., Shi W.D., Li W., Zhang D.S., Jiang X.P., Unsteady numerical calculation and validation on self-priming process of self-priming spray irrigation pump. *Transactions of the Chinese Society of Agricultural Engineering*, 2016, 32(16): 65–72.
- [18] Barrios L., Prado M.G., Modeling two-phase flow inside an electrical submersible pump stage. *Journal of Energy Resources Technology-Transactions of the ASME*, 2011, 133: 042901.
- [19] Stel H., Ofuchi E.M., Sabino R.H.G., Ancajima F.C., Bertoldi D., Neto M.M., Morales R.E.M., Investigation of the motion of bubbles in a centrifugal pump impeller. *Journal of Fluids Engineering-Transactions of the ASME*, 2019, 141: 031203.
- [20] Caridad J., Asuaje M., Kenyery F., Tremante A., Aguillón O., Characterization of a centrifugal pump impeller under two-phase flow conditions. *Journal of Petroleum Science and Engineering*, 2008, 63: 18–22.
- [21] Zhu J.J., Zhu H.W., Zhang J.C., Zhang H.Q., A numerical

- study on flow patterns inside an electrical submersible pump (ESP) and comparison with visualization experiments. *Journal of Petroleum Science and Engineering*, 2019, 173: 339–350.
- [22] Barrios L., Prado M.G., Experimental visualization of two-phase flow inside an electrical submersible pump stage. *Journal of Energy Resources Technology-Transactions of the ASME*, 2011, 133: 042901.
- [23] Shao C.L., Li C.Q., Zhou J.F., Experimental investigation of flow patterns and external performance of a centrifugal pump that transports gas-liquid two-phase mixtures. *International Journal of Heat and Fluid Flow*, 2018, 71: 460–469.
- [24] Limbach P., Skoda R., Numerical and experimental analysis of cavitating flow in a low specific speed centrifugal pump with different surface roughness. *Journal of Fluids Engineering-Transactions of the ASME*, 2017, 139: 101201.
- [25] Kan K., Zheng Y., Chen Y.J., Xie Z.S., Yang G., Yang C.X., Numerical study on the internal flow characteristics of an axial-flow pump under stall conditions. *Journal of Mechanical Science and Technology*, 2018, 32(10): 4683–4695.
- [26] Gu Y.Q., Yu S.W., Mou J.G., Wu D.H., Zheng S.H., Research progress on the collaborative drag reduction effect of polymers and surfactants. *Materials*, 2020, 13(2): 444.
- [27] Gu Y.Q., Yu L.Z., Mou J.G., Wu D.H., Xu M.S., Zhou P.J., Ren Y., Research strategies to develop environmentally friendly marine antifouling coatings. *Marine Drugs*, 2020, 18(7): 371.
- [28] Gu Y.Q., Xia K., Wu D.H., Mou J.G., Zheng S.H., Technical characteristics and wear-resistant mechanism of Nano coatings: a review. *Coatings*, 2020, 10(3): 233.